Supporting Information

Fokina et al. 10.1073/pnas.1007653107

SI Materials and Methods

Overexpression and Purification of Recombinant P_{II} and *N*-Acetyl-Glutamate Kinase (NAGK). The R9L and K58M variants were created with artificial *glnB* genes carrying the respective mutations and cloned into the Strep-tag fusion vector pASK-IBA3 (IBA) after restriction with BsaI as described previously (1). Overexpression of wild-type and mutant *Synechococcus elongatus glnB* in *Escherichia coli* RB9060 (2) and purification of recombinant P_{II} proteins with a C-terminal fused Strep-tag II peptide was performed according to Heinrich et al. (1). His_6-tagged recombinant NAGK from *S. elongatus* was overexpressed in *E. coli* strain BL21(DE3) (3) and purified as reported previously (4).

Surface Plasmon Resonance Detection (SPR). SPR experiments were performed using a BIAcore X biosensor system (Biacore AB) at 25 °C in Hepes-buffered saline (HBS)-Mg buffer containing 10 mM Hepes, 150 mM NaCl, 1 mM $MgCl_2$, and 0.005% Nonidet P-40, pH 7.5 at a flow rate of 15 μL/min as described previously (4). The purified His_6–NAGK was immobilized on the Ni^+-loaded nitrilotriacetate (NTA) sensor chip to flow cell 2 (FC2) in a volume of 50 μL at a concentration of 30 nM (hexamer) to receive a binding signal of approximately 3,000 resonance units (RU), which corresponds to a surface concentration change of 3 ng/mm^2.

In order to analyze the effect of 2-oxoglutarate (2-OG) on the dissociation of WT P_{II}–NAGK complex, 100 nM P_{II} was bound to the His_6–NAGK and then the analyte containing 1 mM ATP and different concentrations of 2-OG diluted in HBS-Mg buffer (50 μL) was injected to both FC1 and FC2 on the sensor chip. The specific binding of P_{II} to NAGK and dissociation was recorded as the response signal difference FC2-FC1.

P_{II} was removed from the His_6–NAGK surface by injecting 25 μL of 1 mM ADP. For novel reload of proteins on the NTA sensor chip, 25 μL of 0.4 M EDTA pH 7.5 was injected to remove His_6–NAGK and Ni^+. Subsequently, the chip could be loaded again with 5 mM Ni_2SO_4 solution and His_6–NAGK as described above.

Isothermal Titration Calorimetry (ITC). ITC experiments were performed on a VP-ITC microcalorimeter (MicroCal, LCC) in buffer containing 10 mM Hepes-NaOH, pH 7.4, 50 mM KCl, 50 mM NaCl, and 1 mM $MgCl_2$ at 20 °C. For determination of ATP- and 2-OG–binding isotherms for P_{II} variants R9L and K58M, different amounts of protein solution (16, 25, or 33 μM trimer concentration) were titrated with 1 mM ATP or 4 mM 2-OG (in the presence of 1 mM ATP). For one measurement 5 μL ligand was injected 35 times in 1.4285 mL cell with stirring at 350 rpm. The binding isotherms were calculated from received data and fitted to a three-site binding model using the MicroCal ORIGIN software (Northampton) as indicated.

Coupled NAGK Activity Assay. Activity of NAGK was determined by coupling NAG phosphorylation via pyruvate kinase and lactate dehydrogenase to the oxidation of NADH. The assay was performed as described previously, the reaction buffer consisting of 50 mM imidazole, pH 7.5, 50 mM KCl, 20 mM $MgCl_2$, 0.4 mM NADH, 1 mM phosphoenolpyruvate, 10 mM ATP, 0.5 mM DTT, 11 U lactate dehydrogenase, 15 U pyruvate kinase, 50 μM arginine, 1.2 μg P_{II}, and 3 μg NAGK (5). The mixture was preincubated for 3 min to allow P_{II}–NAGK complex formation. Then, the reaction was started by the addition of 50 mM NAG and 2-OG (to determine the effect of increasing 2-OG concentrations on disruption of P_{II}–NAGK complex in the presence of NAGK-inhibiting concentrations of arginine). Then 20 s after addition of substrate, the change in absorbance at 340 nm was recorded for 10 min. Linear kinetics were observed over the period of time. Phosphorylation of one molecule of NAG leads to oxidation of one molecule of NADH, which is followed by the linear decrease of absorbance at 340 nm. The reaction was recorded in a SPECORD 200 photometer (Analytik Jena). The reaction velocity was calculated from the slope of the resulting time curve as change in absorbance per time with one unit of NAGK ($e_{\tilde{34}} = 6{,}178\ \mathrm{L\,mol^{-1}\,cm^{-1}}$) catalyzing the conversion of 1 mmol NAG per min.

Crystallization of Recombinant *S. elongatus* P_{II} Protein. Crystallization was performed with the sitting-drop technique by mixing 400 nL of the protein solution with equal amounts of the reservoir solution using the honeybee robot (Genomic Solutions Ltd.). Drops were incubated at 20 °C and pictures were recorded by the RockImager system (Formulatrix). The crystallization buffer was composed of 10 mM Tris (pH 7.4), 0.5 mM EDTA, 100 mM NaCl, 1% glycerol, and 2 mM ATP-Mg, and also 2 mM 2-OG was added; crystals appeared in a precipitant condition containing PEG 4000. Glycerol was used as the cryoprotectant and the crystals were flash-frozen in liquid nitrogen. Diffraction data were collected at the Swiss Light Source. Diffraction images were recorded on a MarCCD camera 225 (Marresearch) and images were processed using the XDS/XSCALE software (6). The structure was solved by molecular replacement using the program Molrep (7). Rebuilding of the structure and structure refinement was performed using the programs Coot and Refmac (8, 9). The quality of the structure was analyzed by the Procheck program (10). Figures were generated using PyMOL (www.pymol.org).

For crystallization of $P_{II}{}^{OG1-3}$ structures, 2-OG-containing P_{II} protein was used. Crystals appeared after 30 d in a precipitant condition containing sodium acetate trihydrate 0.1 M, pH 5, PEG 4000, and 2-methyl-2,4-pentanediol.

1. Heinrich A, Maheswaran M, Ruppert U, Forchhammer K (2004) The *Synechococcus elongatus* P_{II} signal transduction protein controls arginine synthesis by complex formation with *N*-acetyl-L-glutamate kinase. *Mol Microbiol* 52:1303–1314.
2. Bueno R, Pahel G, Magasanik B (1985) Role of glnB and glnD gene products in regulation of the glnALG operon of Escherichia coli. *J Bacteriol* 164:816–822.
3. Studier FW, Rosenberg AH, Dunn JJ, Dubendorff JW (1990) Use of T7 RNA polymerase to direct expression of cloned genes. *Methods Enzymol* 185:60–89.
4. Maheswaran M, Urbanke C, Forchhammer K (2004) Complex formation and catalytic activation by the P_{II} signaling protein of *N*-acetyl-L-glutamate kinase from *Synechococcus elongatus* strain PCC 7942. *J Biol Chem* 279:55202–55210.
5. Beez S, Fokina O, Herrmann C, Forchhammer K (2009) *N*-acetyl-L-glutamate kinase (NAGK) from oxygenic phototrophs: P_{II} signal transduction across domains of life reveals novel insights in NAGK control. *J Mol Biol* 389:748–758.
6. Kabsch W (2010) XDS. *Acta Crystallogr, Sect D: Biol Crystallogr* 66:125–132.
7. Vagin A, Teplyakov A (1997) MOLREP: An automated program for molecular replacement. *J Appl Crystallogr* 30:1022–1025.
8. Murshudov GN, Vagin AA, Dodson EJ (1997) Refinement of macromolecular structures by the maximum-likelihood method. *Acta Crystallogr, Sect D: Biol Crystallogr* 53:240–255.
9. Emsley P, Cowtan K (2004) Coot: Model-building tools for molecular graphics. *Acta Crystallogr, Sect D: Biol Crystallogr* 60:2126–2132.
10. Laskowski RA, Macarthur MW, Moss DS, Thornton JM (1993) Procheck—a program to check the stereochemical quality of protein structures. *J Appl Crystallogr* 26:283–291.

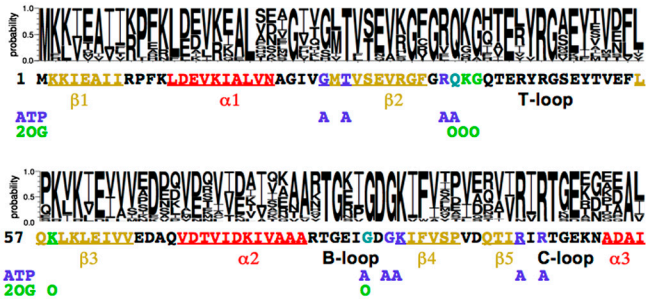

Fig. S1. Primary and secondary structure of the *S. elongatus* P_{II} protein with representation of sequence conservation and indication of amino acids, involved in ATP and 2-OG binding. Below the amino acid sequence of the *S. elongatus* P_{II} protein (middle line), the secondary structure elements and T, B, and C loops are indicated; α-helices and β-strands are underlined and colored in red or in brown, respectively. The position of amino acids involved in ATP binding (blue), 2-OG binding (green), or both (cyan) are highlighted with A or O (the coloring of these amino acids overrides the coloring of secondary structure elements). On top, the amino acid sequence conservation is represented as a sequence logo, derived from multiple sequence alignment of 14 different P_{II} proteins from the major prokaryotic lineages. The sequence logo was created with the program WebLogo 3.0. (http://weblogo.threeplusone.com/). The frequency of an amino acid in the multiple alignment is represented by the height of the letter. Multiple sequence alignment was carried out with the program ClustalW (http://www.ebi.ac.uk/Tools/clustalw2/) using the following P_{II} sequences (Gene Bank accession numbers in parentheses): *S. elongatus* (YP_171902.1); *Nostoc* sp. strain 7120 (BAB74018.1); *Prochlorococcus marinus* MIT 9301 (YP_001091877.1); *Thiobacillus denitrificans* ATCC25259 (AAZ96761.1); *E. coli* GlnB (AAB28779.1); *E. coli* GlnK (CAQ30923.1); *Azospirillum brasiliense* GlnB (AAK01659.1); *A. brasiliense* GlnK (ADK11050.1); *A. brasiliense* GlnZ (AAG10012.1); *Bacillus subtilis* GlnK (AAA17400.1); *Lactococcus lactis* subsp. cremoris MG1363 (AAX82491.1); *Streptomyces coelicolor* A3 (NP_733668.1); *Methanococcus maripaludis* GlnB (CAF29622.1); *Methanocaldococcus jannaschii* DSM 2661 GlnB (AAB98041.1).

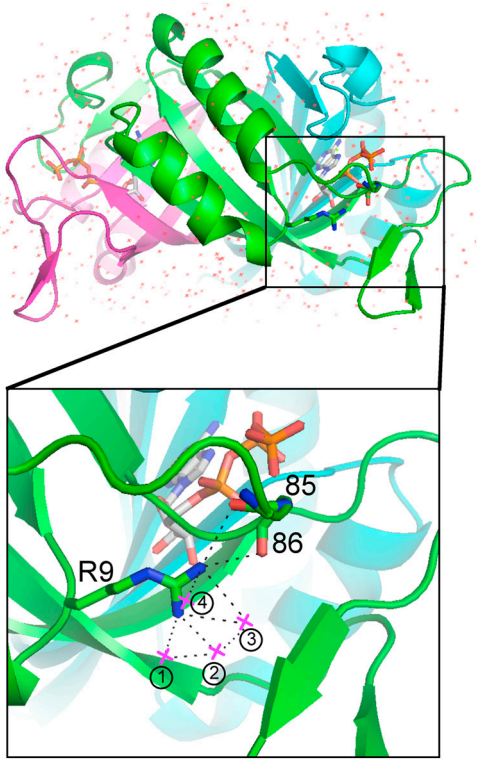

Fig. S2. Role of R9 residue in stabilizing the active site of P_{II} in the NAGK-binding conformation. Ribbon presentation of the structure of the P_{II} I86N variant (mimicking the NAGK-binding conformation) with unbound water molecules. ATP and relevant side- or main-chain residues are shown in sticks; black broken lines indicate contacts between R9 and main-chain oxygens of B-loop residues or water molecules that are designated 1, 2, 3, and 4. One of these water molecules (2) makes contact with T-loop backbone oxygen of R45 (2.80 Å), water 3 with the carboxyl group of E85 (2.83 Å), and water 4 also with E85 (2.66 Å) and the hydroxyl group of T83 (2.84 Å).

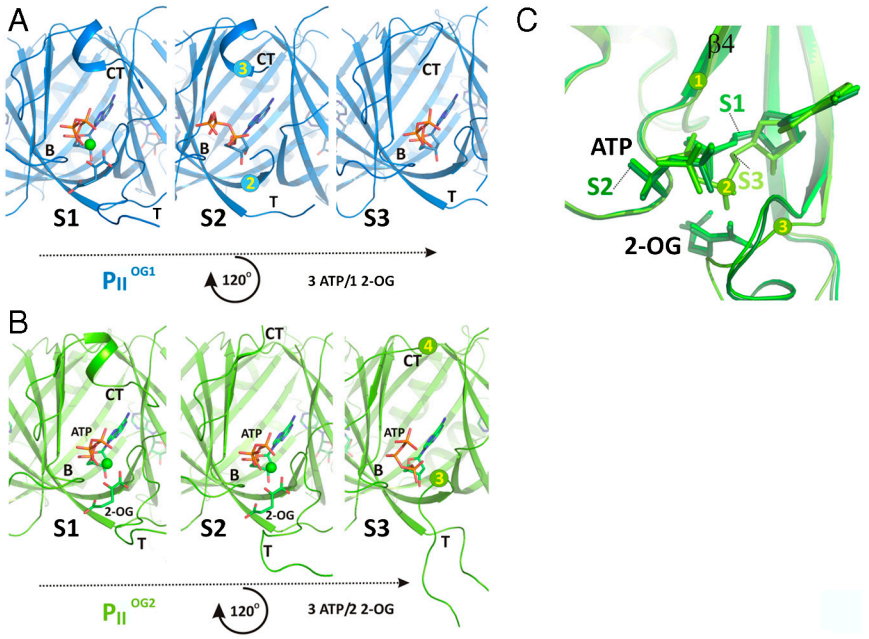

Fig. S3. Comparison of effector molecule-binding sites between P_{II}^{OG1} and P_{II}^{OG2}. (*A*) Ribbon representation figure identical to Fig. 3*C* (this paper) for comparison. (*B*) Ribbon representation of the P_{II}^{OG2} structure with a view into the three ligand-binding sites (S1, S2, and S3). Cofactors as well as the B loop, T loop, and C terminus are marked and the composition of the complex is marked below the structure figure. Significant structural changes between the three monomers are marked in S3 with encircled numbers (3, T loop; 4, C terminus). (*C*) Superposition of the three monomers of P_{II}^{OG2} and zoom into the ligand-binding pocket with the ligands of one monomer color coded in different greens. Significant changes are visible in the ATP conformation (marked with 2), in the T-loop conformation (marked with 3), and in strand β4 with residues contributing to ATP and 2-OG complexation located close to the binding site (marked with 1).

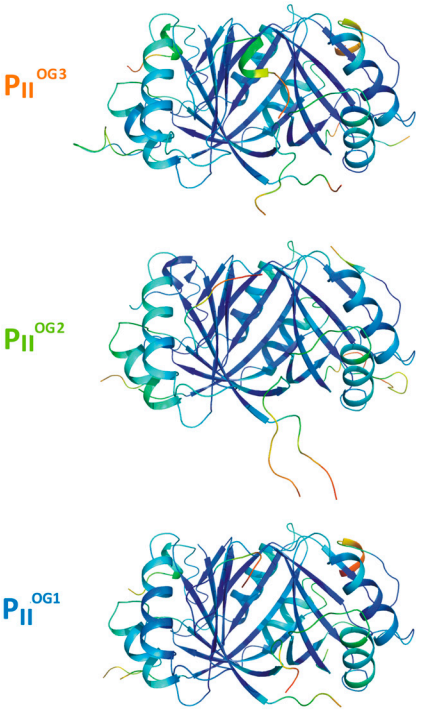

Fig. S4. Representation of the *B* factors in structures P_{II}^{OG1}–P_{II}^{OG3} with blue color indicating lowest *B* factors and red color highest temperature factors. The structures indicate that binding of the 2-OG ligand does not induce major changes in the protein flexibility and thereby the *B* factors.

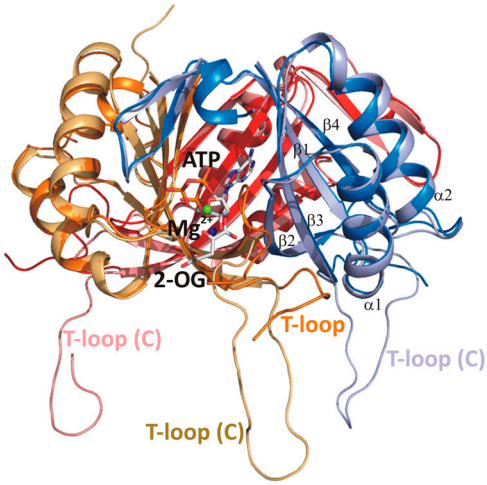

Fig. S5. Superposition of the P_{II}^{OGex} structure with the structure of P_{II} in complex with PipX [Protein Data Bank (PDB) ID code 2XG8] as ribbon models. The color code for the P_{II}^{OGex} structure is derived from Fig 1*B*, and that for P_{II} from the P_{II}–PipX complex is adapted. Secondary structure elements are marked. ATP and 2-OG are shown in stick representation whereas the Mg^{2+} ion is marked in green. The T loop from the P_{II}–PipX complex structure, labeled as "T loop (C)", displays a vertically extended conformation, which retracts upon 2-OG binding.

Table S1. Data collection and refinement statistics

	P_{II}^{OGex}	$P_{II}^{OG1–3}$
Data collection		
Space group	$P2_12_12_1$	$P22_12_1$
Cell dimensions		
a, *b*, *c*, Å	71.87, 87.99, 116.34	72.33, 102.37, 135.77
α, β, γ, °	90	90
Resolution, Å	29 – 2.2 (2.33-2.2)	48 – 1.95 (2.06-1.95)
R_{sym} or R_{merge}	0.12 (0.78)	0.12 (0.85)
$I/\sigma I$	13.3 (2.6)	12.2 (1.8)
Completeness, %	99.6 (98.1)	98.1 (94.1)
Redundancy	7.2 (7.1)	7.1 (6.9)
Refinement		
Resolution, Å	29 – 2.2 (2.25-2.2)	48 – 1.95 (2-1.95)
No. reflections	36239 (2522)	69753 (3672)
R_{work}/R_{free}	0.18/0.22 (0.22/0.29)	0.17/0.22 (0.22/0.29)
No. atoms (all)	5433	8101
Protein (chains/residues)	6/646	9/965
Ligands (ATP/αKG/CIT/Mg^{2+})	6/6/-/6	9/7/-/7
Water	248	318
B factors		
Protein	22	24.6
Ligand/ion (ATP/αKG/CIT/Mg^{2+})	22.4/31.1/-/29.6	22.5/27.6/-/23.4
Water	59	59.4
rmsd		
Bond lengths, Å	0.029	0.025
Bond angles, °	2.1	2.2
Ramachandran statistics		
No. of residues in favored region (%)	605 (97.4)	912 (97.7)
No. of residues in allowed region (%)	16 (2.6)	21 (2.3)
No. of residues in outlier region (%)	0	0
PDB ID code	2XOH	2XOJ

Values in parentheses are for the highest-resolution shell.

Table S2. Molecular interface analysis of the subunits in the P_{II}^{OG1-3} structure (values are given in $Å^2$)

	A	B	C
P_{II}^{OG1}			
A		1,200	1,180
B	1,200		1,070
C	1,180	1,070	
P_{II}^{OG2}			
A		1,210	1,190
B	1,210		1,090
C	1,190	1,090	
P_{II}^{OG3}			
A		1,260	1,250
B	1,260		1,160
C	1,250	1,160	